1 Fundamentals

1.1 Introduction

A mass spectrometer is an instrument for generating gas-phase ions, separating them according to their mass-to-charge ratio using electric fields (sometimes magnetic fields as well) in an evacuated volume, and counting the number of ions. A computer system controls the operation and stores, manipulates and presents the data. The features of the mass spectra so produced relate to the properties of the original sample in a well understood way. This chapter deals with some of the fundamental aspects of mass spectrometry: how samples are introduced to the instrument (inlets); how the ions are fragmented; how ions are counted (detectors) and the type of output and how it is manipulated (data systems and data processing) and interpreted (isotope patterns). How the ions are separated (mass analysers) is dealt with in Chapter 2 and the how the ions are formed (ionisation techniques) in Chapter 3.

Figure 1.1 is a schematic drawing of a mass spectrometer. The sample is introduced through an inlet to the ionisation source. The source generates gas-phase ions, which are transferred to the mass analyser for separation according to their mass-to-charge ratio. A detector registers and counts the arriving ions. The data system controls the various components of the mass spectrometer electronically, and stores and manipulates the data. All mass spectrometers have a vacuum system to maintain the low pressure (high vacuum) required for operation. High vacuum minimises ion-molecule reactions as well as scattering and neutralisation of the ions.

Modern instruments often have the facility to perform more than one mass analysis on a single sample, i.e. MS/MS or even MS^n (where n = number of stages of mass spectrometry). Such machines require more than one mass analyser, or alternatively, have the facility to trap ions in a small volume of space and carry out repeated experiments on them. Both types of mass spectrometer require the ability to fragment ions, and this is usually achieved by collision-induced dissociation, another topic covered in this chapter.

1.2 Inlets

The way in which a sample is introduced to the mass spectrometer is very dependent on its phase (gas, liquid, solid or solution) and the means by which ionisation is induced. Gaseous samples are easily transferred to a mass spectrometer, as the gas may simply be allowed to leak into the low pressure source region. The effluent from the capillary

Mass Spectrometry of Inorganic, Coordination and Organometallic Compounds W. Henderson and J. S. McIndoe
 ISBNs: 0-470-85015-9 (HB); 0-470-85016-7 (PB)

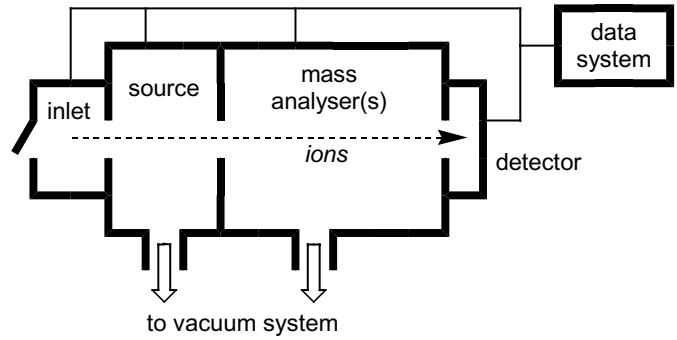

Figure 1.1
Schematic of a mass spectrometer

column of a gas chromatograph (GC) may be conveniently plumbed directly into the source of a mass spectrometer. Condensed phase analytes (liquid or solid) are placed on a sample holder and passed through a door into the instrument. The door is closed, sealed and the inlet/source region is evacuated, after which time whatever ionisation technique being used is applied. Analytes dissolved in a solvent are usually introduced to the mass spectrometer *via* a combined inlet/ionisation source, in which sample introduction, desolvation and ionisation are intimately related. The solution is commonly the effluent from a liquid chromatograph (LC), or it may be injected directly into the instrument by means of a syringe pump.

1.3 Collision-Induced Dissociation[1]

Collision-induced dissociation (CID, sometimes known as collision-*activated* decomposition, or CAD) of ions occurs when some of the translational energy of an accelerated ion is converted into internal energy upon collision with a residual gas (typically nitrogen or one of the noble gases helium, argon, xenon). The increase in internal energy can induce decomposition (fragmentation) of the ion. CID was of limited importance in mass spectrometry – indeed, some instruments were fitted with 'metastable suppressors' designed to eliminate this troublesome effect – until the advent of soft ionisation techniques. The ability of these techniques to obtain practically intact molecular ions for many classes of compound was enormously useful in itself, but obtaining structural information through characteristic fragmentation patterns is also highly desirable and CID proved to be the ideal answer to this problem.

The first step in the CID process is the actual collision between a fast-moving ion and an immobile neutral target, resulting in an increase in the internal energy of the ion. The ion then rapidly redistributes this extra energy amongst its vibrational modes, which number $3N - 6$ for an ion with N non-linear atoms. The much slower second step is the unimolecular decomposition of the excited ion to generate product ions and neutral fragments. Because the timescale of the first step is very much shorter than the second, large ions are more difficult to fragment using CID as they have more vibrational modes in which to deposit the extra energy, making decomposition of the ion less likely. Two collision regimes for CID may be defined, low energy (tens of electron volts (eV)) and high energy (thousands of eV).

In practice, low-energy CID is carried out by allowing an accelerated beam of ions to traverse a volume occupied by gas molecules or atoms as the target. In MS/MS

instruments in which the mass analysers are separated in space, such as the triple quadrupole $(QqQ)^2$ or hybrid quadrupole-Time-of-flight (QqTOF), an rf-only quadrupole (the 'q' in QqQ) encloses this volume, called a **collision cell**. The directional focusing abilities of the rf-only quadrupole are used to good effect here, redirecting ions back on to the right axis after collisions drive them off-course. However, the potential well created by a rf-only quadrupole field is not particularly steep-sided and ion losses do occur. Better ion guides are rf-only hexapoles or octapoles and the recently introduced **ion tunnels**. The latter are a series of ring shaped, alternately charged electrodes, 60 or more of which describe a hollow cylinder inside of which the ions are tightly confined. Whatever its configuration, the collision cell is separated from the mass analysers either side by narrow apertures and is filled with an inert gas. Ions emerging from the first mass analyser are fragmented (and often scattered) upon collision with the gas, strongly refocused back on to the ion optical axis by the rf-only field, transmitted to the second mass analyser and then detected. A large number of collisions is allowed to occur in the collision cell, so collision yields (the percentage of fragmented ions that reach the detector) are frequently very high for this form of CID. In MS/MS instruments that rely on each stage of MS being carried out sequentially (*in time*) in the same space, such as ion traps or Fourier Transform Ion Cyclotron Resonance (FTICR) analysers, the collision gas is simply introduced to the chamber. The ions are energised and fragmented by CID. The process is especially simple for ion traps, which typically contain a background pressure of helium gas at about 10^{-3} mbar during operation, so the trap does not even need to be filled and emptied between stages of MS/MS.

The nature of the target gas is important in low-energy CID. A large proportion of the translational energy of the ion is transformed into internal energy upon collision with an effectively stationary target, the mass of which has a significant effect on the spectra (so the extent of dissociation increases $He < Ar < Xe$). Atomic gases are more efficient than polyatomic gases in causing CID, because the latter can be vibrationally excited themselves upon collision and hence reduce the amount of energy transferred to the ion. The chemical effects of the target are also important due to the possibility of ion/molecule reactions, so if dissociation of the precursor ion only is sought, an inert target gas is desirable (making the noble gases doubly appropriate). However, there are some circumstances in which ion/molecule reactions are of great interest.

Low-energy CID spectra are very sensitive to small absolute changes in the collision energy, to collision gas pressure and to the mass of the neutral target. These factors conspire to make the reproducibility of low-energy CID spectra between instruments poor compared to electron ionisation mass spectra, for which searchable libraries of spectra are very well established.

Instruments with an atmospheric pressure source have another region in which low-energy CID can occur, located just before the ions enter the high-vacuum region of the mass spectrometer. Here, the pressure is low enough that the mean free path length of the accelerating ions is sufficiently long that they can attain a high enough velocity for collisions with residual solvent molecules and/or desolvation gas to cause fragmentation. This process is called **in-source** CID, and is an especially important facility for instruments with a single mass analyser. The ions are accelerated by application of a variable voltage between the sampling cone and the skimmer cone (which separate differentially pumped regions of the instrument; Chapter 3, Section 8 on electrospray ionisation gives more details), and this 'cone voltage' generally has the most profound effect on the mass spectrum of any of the parameters used to tune the instrument.

High-energy CID is the preserve of sector instruments (Chapter 2, Section 2), which accelerate and analyse ions with energies of thousands of eV. rf-only multipoles are useless as collision cells under these circumstances, as they are unable to refocus such energetic ions after a collision. A simple reaction region containing the collision gas is quite sufficient; ions deflected more than a few tenths of a degree upon collision are lost. The lack of means by which to refocus errant ions and a peak-broadening effect due to kinetic energy release upon collision conspire to make high-energy CID markedly less efficient in terms of conversion of precursor ion to *detected* product ion than its low-energy cousin. The distribution of energies transferred at collision energies of thousands of eV is broad, and high-energy processes result in some product ions that do not appear at all in low-energy CID spectra.

1.3.1 Bond Dissociation Energies from CID Studies

Bond dissociation energies may be obtained from low-energy ('threshold') CID studies, by analysing the kinetic energy dependence of the reactions of metal complexes with an inert collision gas,[3] and ion thermochemistry remains an active research field.[4] Threshold CID experiments are carried out using guided ion beam mass spectrometers, custom-made instruments that allow the sequential generation, thermalisation (cooling), mass selection, fragmentation and mass analysis of ions.[5] To obtain precise data, multiple ion-neutral collisions are eliminated, careful consideration is taken of internal energies of the complexes and their dissociation lifetimes, and the experiments are backed up by Density Functional Theory (DFT) calculations. Fundamental information such as the stepwise energies for dissociation of $[Pt(NH_3)_x]^+$ ($x = 1 - 4$) or $[Cr(CO)_x]^+$ ($x = 1 - 6$) complexes can be obtained using this approach.[6] The main limitation for wider applicability of this technique is that experiments cannot yet be implemented on commercially available instruments. Metal-ligand bond dissociation energies have also been established using FTICR experiments under single-collision conditions.[7]

1.3.2 Presentation of CID Data

Detailed CID investigation of a compound can generate huge quantities of data – in a typical low-energy CID experiment, the collision energy can be varied from 0 – 200 eV, and the analyst must decide which spectra are most representative and informative. This is traditionally carried out by means of a stacked plot, selecting values for the collision energy so that all product ions show up in at least one of the spectra chosen. Numerous examples of this approach can be seen in Chapters 4 to 7 (*e.g.* Figures 4.3, 4.6, 5.6, 5.8 etc.).

If the appearance/disappearance potentials of a particular ion are of special interest, the breakdown graph is an effective way of presenting this data.[8] A breakdown graph plots the intensity of a given ion against the fragmentation energy, represented by the cone voltage (for in-source CID) or collision voltage (for CID in a collision cell). Multiple ions may be presented on a single breakdown graph (Figure 1.2).

In more complicated cases, where there are many fragment ions, and/or a mixture of ions, it may be beneficial to collect spectra across the entire energy range and present all the information simultaneously. This approach is encapsulated in energy-dependent electrospray ionisation mass spectrometry (EDESI MS), which uses a presentation style reminiscent of two-dimensional NMR spectra.[9] The precursor and all product ions appear as cross-peaks in a contour map, where the contours represent ion intensity. The approach is best illustrated with an example (Figure 1.3).

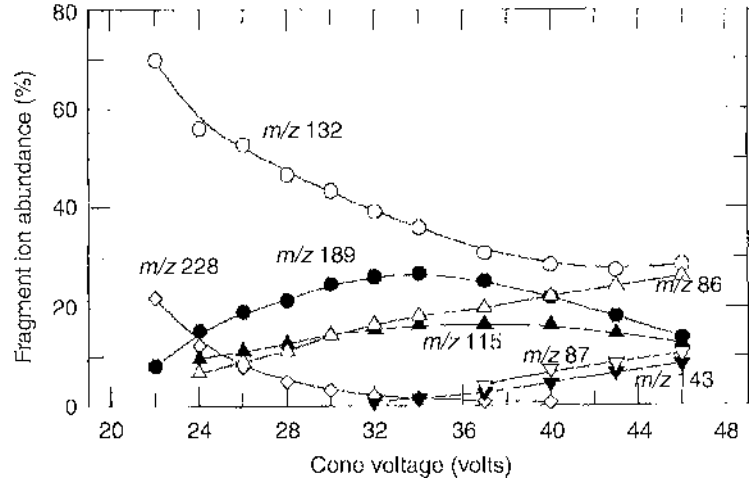

Figure 1.2
Breakdown graphs obtained by CID of protonated H-Gly-Gly-Leu-OH. From Harrison. Reproduced by permission of Wiley Interscience

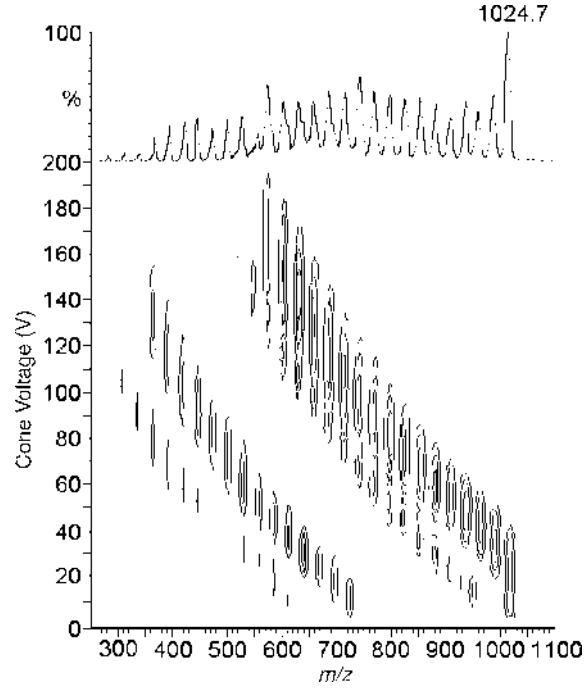

Figure 1.3
EDESI mass spectrum of a mixture of four anionic metal carbonyl clusters, $[Ru_5CoC(CO)_{16}]^-$, $[HRu_4Co_2C(CO)_{15}]^-$, $[Ru_3Co(CO)_{13}]^-$ and $[RuCo_3(CO)_{12}]^-$.[10] Note how each component of the mixture is clearly discriminated in the map, but the summed spectrum at the top is uninformative

1.4 Detectors

The abundance of ions at each mass-to-charge ratio (*m/z*) value must be measured, and this is the role of the **detector**. The ideal detector will have a wide dynamic range (able to detect a few ions arriving just as well as tens of thousands) and a response as linear as possible (provide a peak 100 × larger for 1000 ions than that produced for 10). In the earliest days of mass spectrometry detectors were simply photographic paper but this method was essentially made obsolete by the introduction of electron multipliers. These devices convert the kinetic energy of the arriving particles into electrical signals. The incoming ions strike a surface called a dynode, which is capable of releasing one or more electrons when struck by a particle having an energy above a certain level. Usually, there are a series of dynodes and the released electron is accelerated towards the second dynode, which releases further electrons (Figure 1.4). By repeating this input and release process many times, the number of electrons increases in a geometrical progression (10^6 to 10^8 ×).

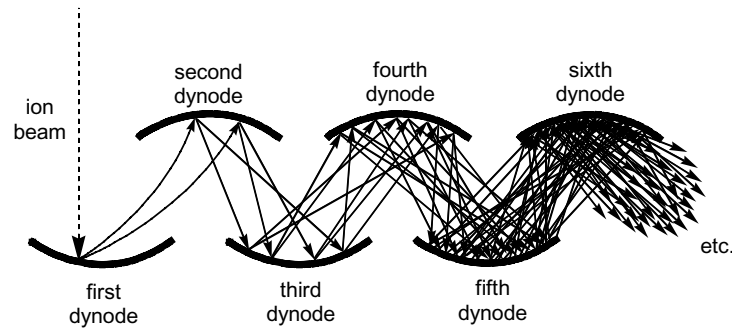

Figure 1.4
An electron multiplier. An ion travelling at high speed causes secondary electrons to be ejected from a metal surface (a dynode) upon impact. These electrons are accelerated through an electric potential towards a second dynode, releasing more electrons, and so on until a blizzard of electrons strikes the final dynode, producing a detectable current which may be amplified further

A scintillator or 'Daly detector' accelerates the secondary electrons (generated when the incoming ions strike the first dynode) towards a dynode made of a substance that emits photons (a phosphor). A photomultiplier tube enhances the signal which is ultimately converted into an electric current. This arrangement has some advantages over the electron multiplier as the photomultiplier may be sealed from the vacuum of the mass spectrometer and does not suffer ill effects from the presence of residual gas or discharged ions, significantly increasing the lifetime of the detector.

In some applications it is advantageous to collect ions over an area using an **array detector**, rather than a point detector which relies on ions arriving sequentially at a single location. Array detectors can detect ions arriving simultaneously at different points in space. This property is particularly useful in sector instruments, which disperse ions in space, so a number of detectors arranged in a line are capable of measuring a section of the mass spectrum in the same amount of time that a single detector can measure a single *m/z* value. For example, an array detector containing ten collectors could simultaneously

measure ten times the mass range that a single collector could in the same time. The efficiency of detection is thus greatly improved, important in applications requiring high sensitivity.

TOF instruments generate a pulse of ions of a wide range of *m/z* values, all of which arrive at the detector within a few microseconds, and ions of adjacent *m/z* value are separated in time by less than a nanosecond. A detector is required that has a very fast recovery time. Furthermore, orthogonal-TOF mass analysers pulse a whole section of an ion beam at once, and this spatial dispersion in the original direction of travel is preserved as the ions progress down the flight tube. The ions arrive at the detector across a broad front, demanding a detector able to accept ions over an equally wide area. Both of these obstacles are solved by the use of a **microchannel plate** (MCP), which consists of a large number (thousands) of tightly packed individual detection elements all connected to the same backing plate. Each of these 'microchannels' is a tiny electron multiplier tube, and an ion arriving in any of them sets off a cascade of electrons to provide a detectable signal. A **time-to-digital converter** (TDC) sets up timing increments separated by intervals of less than a nanosecond, and a signal detected in any of these intervals is recorded as an arrival time. It does not, however, record the intensity of the signal, so two ions arriving with the same time interval on different parts of the MCP are still recorded as a single arrival time. Generally, this does not pose a problem; a TOF analyser is typically recording 30 000 spectra per second so the number of ions arriving in any one individual spectrum is low. However, it becomes an issue when recording particularly high ion currents, and is exacerbated by the fact that the TDC itself has a 'dead time', in which it takes some time to recover before it can record a new event. These effects conspire to affect the quantitative response of TOF detectors, and high ion currents tend to distort peak shape and underestimate intense signals, though computer processing does mitigate the detrimental effects to a large degree.

1.5 Mass Resolution

The resolution of a mass spectrometer represents its ability to separate ions of different *m/z*. It is manifested in the sharpness of the peaks seen in the mass spectrum. An instrument with high resolving power will be able to distinguish two peaks very close in mass. Calculating the resolution is done in one of two ways. Magnetic instruments tend to give peaks which are essentially Gaussian in shape, and the usual definition is $R = m/\Delta m$, where m is the mass of an ion peak and Δm is the distance to another peak overlapping such that there is a 10 % valley between the two peaks (Figure 1.5).

In the figure, $m = 1000$ and $\Delta m = 0.208$, so the 10 % valley definition gives a resolution of $1000/0.208 = 4800$. It is generally more convenient to conduct the calculation on a single ion, in which case Δm is the full width of the peak at 5 % of its maximum intensity. Another common resolution calculation uses the full width of the peak at half maximum intensity (FWHM). This definition is commonly used for TOF and ion trap instruments, which typically have relatively broad-based peak profiles and as such the 5 % definition exaggerates the peak width and hence gives an unreasonably low value for the resolution. In the figure shown, FWHM = 1000/0.1 = 10 000. Clearly, when comparing resolution performance between instruments it is important to apply the same definition in each case. Generally in this text, 'resolution' will correspond to the FWHM definition unless otherwise stated.

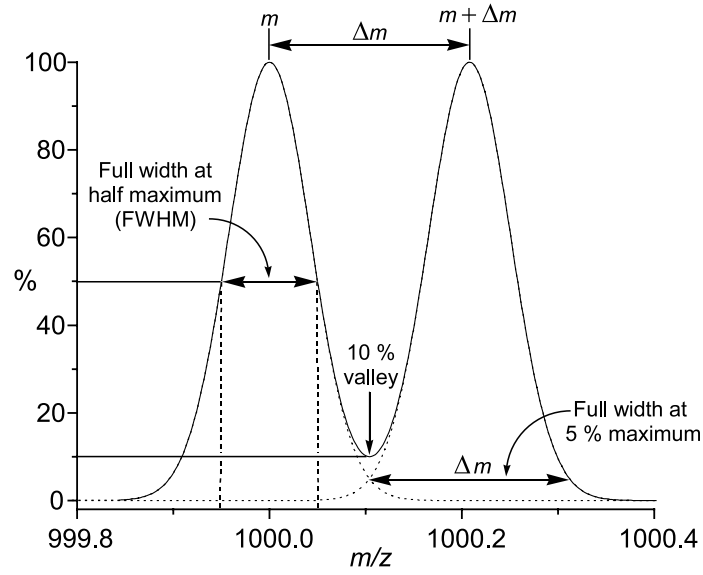

Figure 1.5
Measurements used in calculations of resolution. The FWHM definition will be used in this book

The ability of instruments with different resolution to differentiate between low-mass ions of the same nominal mass is illustrated in Figure 1.6. At low resolution (1000, e.g. quadrupole/ion trap in low resolution mode or linear TOF), the three ions are not discriminated at all and just a single peak is observed. At slightly higher resolution (2500, e.g. quadrupole/ion trap in maximum resolution mode) the higher *m/z* ion is differentiated, but the remaining two ions appear as just a single peak at an *m/z* value intermediate between the two real values. Three peaks can be clearly observed at a resolution of 5000 (e.g. reflectron TOF), and the signals are baseline resolved at 10 000 resolution (e.g. magnetic sector, high performance reflectron TOF, FTICR).

However, the major criterion for an inorganic/organometallic chemist should be the ability to provide good baseline-resolved isotope patterns in the *m/z* range of most interest. The need for high resolution becomes less stringent when it is isotope pattern information that is required. Baseline resolution of the individual members of the isotopomer envelope is the most important criterion for satisfactory data. The majority of coordination complexes and organometallic compounds are below 1000 Da, at which a resolution of 2500 is generally sufficient for good data (Figure 1.7).

However, a resolution much below 2500 will drastically reduce confidence in assignment, as can be clearly seen in the lumpy, indistinct and unsatisfactory profile observed for the spectrum collected at a resolution of 1000. Higher resolution than 2500 is always desirable, especially when collecting data on ions of mass > 1000 Da and for multiply charged ions, and the higher quality the data the correspondingly higher confidence can be had in assignment. A resolution of 2500 can be achieved for practically all modern research level instruments, regardless of type – even relatively inexpensive ion trap and quadrupole machines can be scanned slowly over the isotope envelope region (usually not

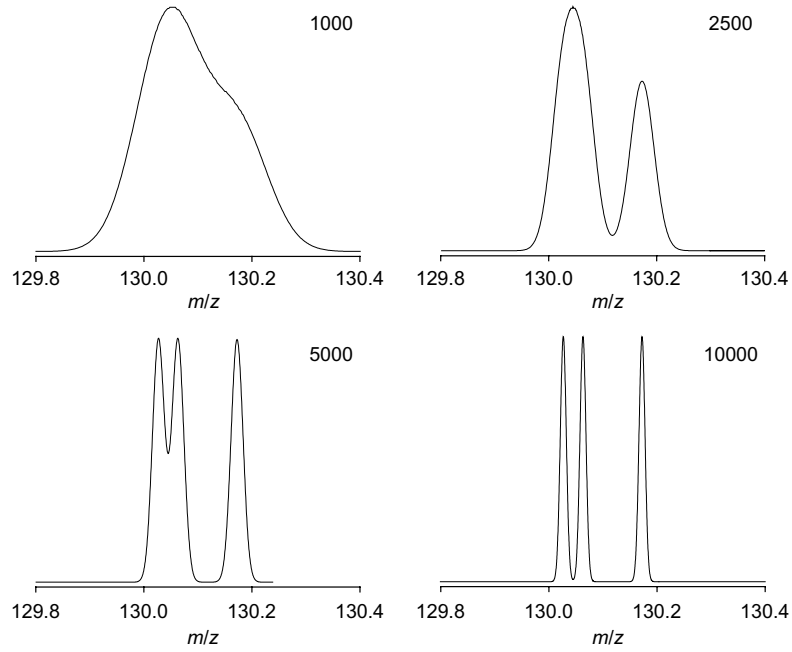

Figure 1.6
Effect of increasing resolution in differentiating the ions $[C_5H_6O_4]^+$, $[C_6H_{10}O_3]^+$ and $[C_9H_{22}]^+$, all with a nominal mass of 130 Da and present in equal amounts. Monoisotopic masses are 130.0266, 130.0630 and 130.1722 *m/z* respectively

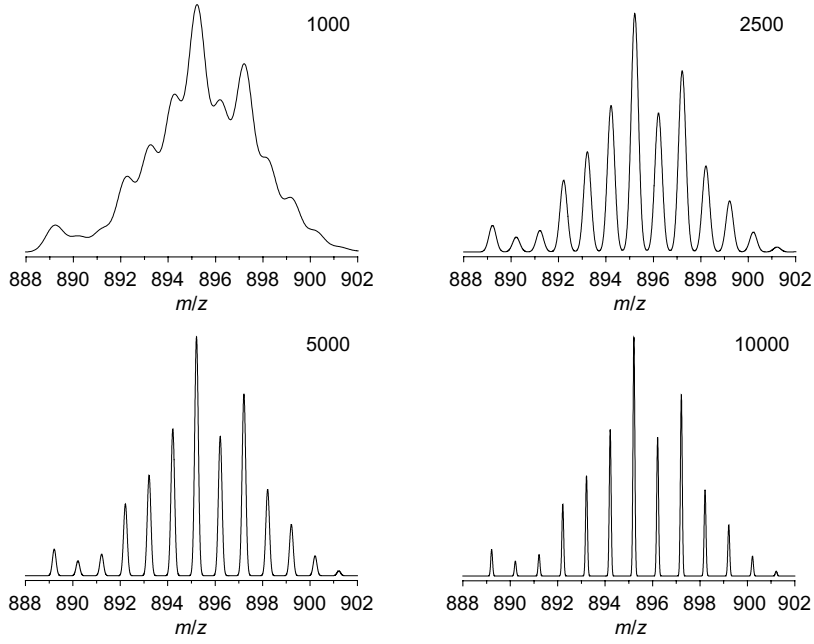

Figure 1.7
Effect of increasing resolution on the isotope pattern for $[C_{51}H_{53}ClP_3Ru]^+$

more than 20 *m/z* wide) to push the resolution up (though there is always a trade-off between resolution and intensity).

1.5.1 Mass Accuracy

The mass accuracy of a spectrometer is the difference observed between the calculated mass of an ion and its observed mass, $\Delta m = m_{\text{calculated}} - m_{\text{observed}}$, expressed relative to the observed mass. It is usually reported in parts per million (ppm):

$$\text{Mass accuracy (ppm)} = 10^6 \times \Delta m / m_{\text{observed}}$$

Careful calibration in conjunction with a reference compound enables high resolution mass spectrometers to provide a mass accuracy of 5 ppm or better. Instruments capable of this are said to provide **accurate mass** data. The requirement for high resolution becomes obvious if we consider again our four hypothetical mass spectrometers (Figure 1.8).

For low resolution mass spectrometers, the peak width is so broad that reliably picking the maximum value to within the required limits is fraught with error, though sound experimental protocols can allow surprisingly good results.[11] Resolution is must be at least 5000 for an instrument to realistically claim the ability to collect accurate mass data, and resolution of 10 000 is desirable. The rate of digitisation is also an issue (Figure 1.9).[12]

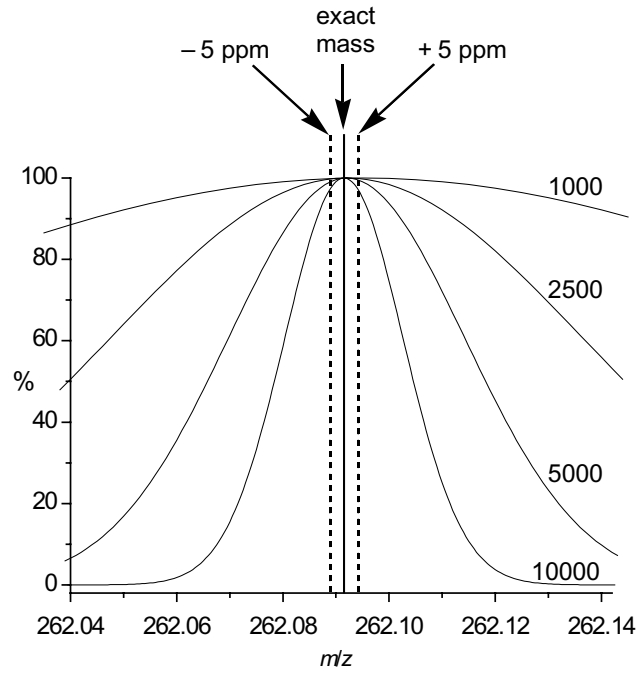

Figure 1.8
Peak profiles for $[C_{18}H_{15}P]^+$, exact mass 262.0911, at resolutions of 1000, 2500, 5000 and 10 000. The dotted lines correspond to the 5 ppm error limits

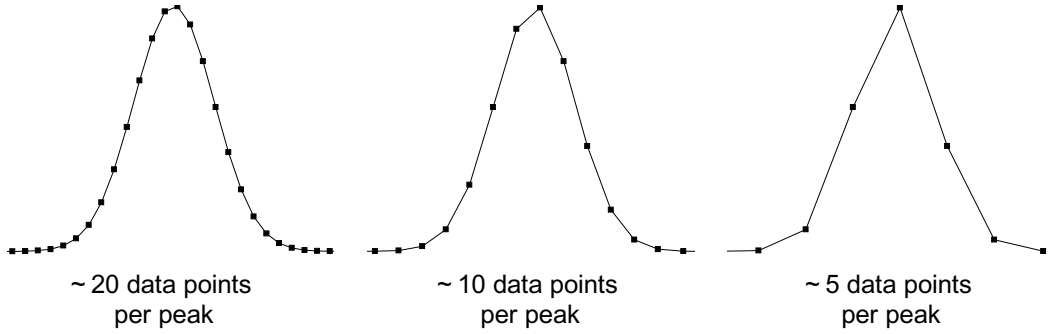

Figure 1.9
The effect of low rates of digitisation on reconstruction of a peak – at least 12 data points across the width of the peak is recommended

A distorted peak shape due to poor tuning or any contribution from an overlapping (isobaric) ion will also detrimentally affect the ability of the instrument to generate an accurate centroid.

Accurate mass data can unambiguously determine the elemental composition of an ion, but this statement comes with some important caveats. First, the number of possible combinations of elements that can fit within a given ppm range increases exponentially with *m/z*. Second, the elements chosen must consist of a severely reduced subset (often just carbon, hydrogen, oxygen and nitrogen plus any other possibilities based on the history of the sample). The elemental composition predicted is reasonably reliable for organic compounds with $m/z < 500$, but becomes increasingly suspect as the mass increases, as a search[13] for matching elemental formulae (limited to C,H,O,N) for increasing *m/z* values demonstrates:

m/z	100.1	200.2	300.3	400.4	500.5	600.6	700.7	800.8	900.9	1001.0
Matches within 5 ppm	1	1	2	2	2	3	4	10	50	139

Historically, the low mass/limited composition restriction posed few problems, as the vast majority of compounds that could be successfully transferred into the gas phase fitted this description. However, with the advent of new ionisation techniques, ions of higher mass and of almost limitless elemental composition can be analysed with ease. Blind faith in the reliability of a match between experimental data and theoretical composition is ill-advised, and in most cases, a well-matched isotope pattern provides more compelling evidence for a correct match.

For example, a minor product isolated from the reaction of $Na[Fe(CO)_2Cp]$ with an R_3SiCl compound provided the isotope pattern reproduced in Figure 1.10. No sensible match for the exact mass of 555.9030 Da using the elements carbon (C), hydrogen (H), oxgyen (O), chlorine (Cl), iron (Fe), and sodium (Na) can be obtained, and extending the search to the whole periodic table resulted in an enormous number of hits. However, comparison of the isotope pattern with various possible elements quickly led to the identification of mercury (Hg) as the likely culprit.

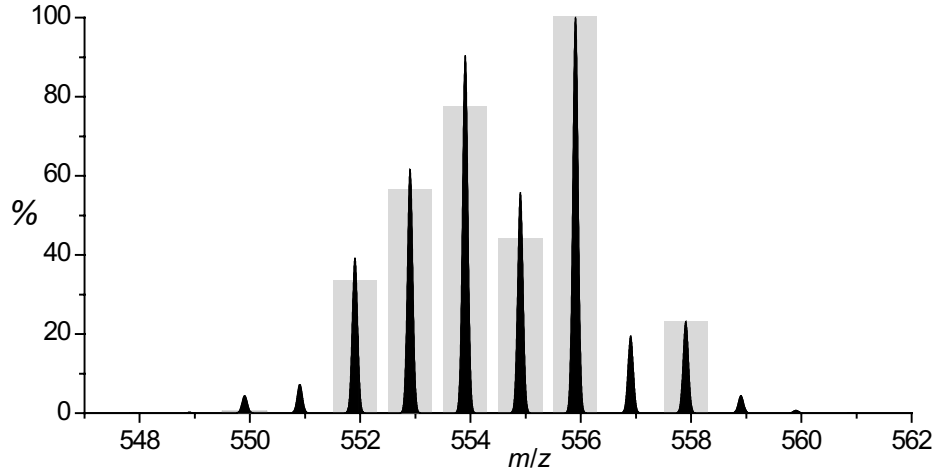

Figure 1.10
The isotope pattern for $[Hg\{Fe(CO)_2Cp\}_2]^+$ superimposed on isotopic signature for Hg. Note the dominant effect the seven isotopes of Hg have on the pattern. Inclusion of the remaining elements Fe, C, H and O in the calculation gave an exact match

The mercury came from inadvertent introduction of some sodium/mercury amalgam used to prepare $Na[Fe(CO)_2Cp]$ from $[Fe(CO)_2Cp]_2$. The usefulness of the isotope pattern over the exact mass measurement is clear in this case, and most inorganic and coordination chemists will find this to be true in nearly all instances.

1.6 Data Processing

The software used for controlling a modern mass spectrometer has powerful abilities to alter the appearance of the raw data collected from an experiment. The raw data may display much noise, an elevated baseline, a curved baseline, and contain a relatively low ratio of useful information to total information. The various data manipulation functions of the software are designed to address one or more of these 'problems'. Three main steps can be applied which affect the appearance of the raw data: smoothing, subtracting and centering (Figure 1.11).

Smoothing

Raw data may be smoothed easily using the mass spectrometry software. One type of algorithm used is the 'moving average' method, which converts each point to a new value generated by averaging it and the n points either side of it. The greater the value of n ($2n + 1$ is called the 'filter width'), the more intense the smoothing effect. This approach is deceptively impressive, and information is lost or distorted because too much weight is given to points far removed from the central point. An improvement is the **Savitsky-Golay** algorithm,[15] which is a computationally efficient way to perform a least-squares fit of the data to a polynomial function. The smoothing effect is less aggressive than the

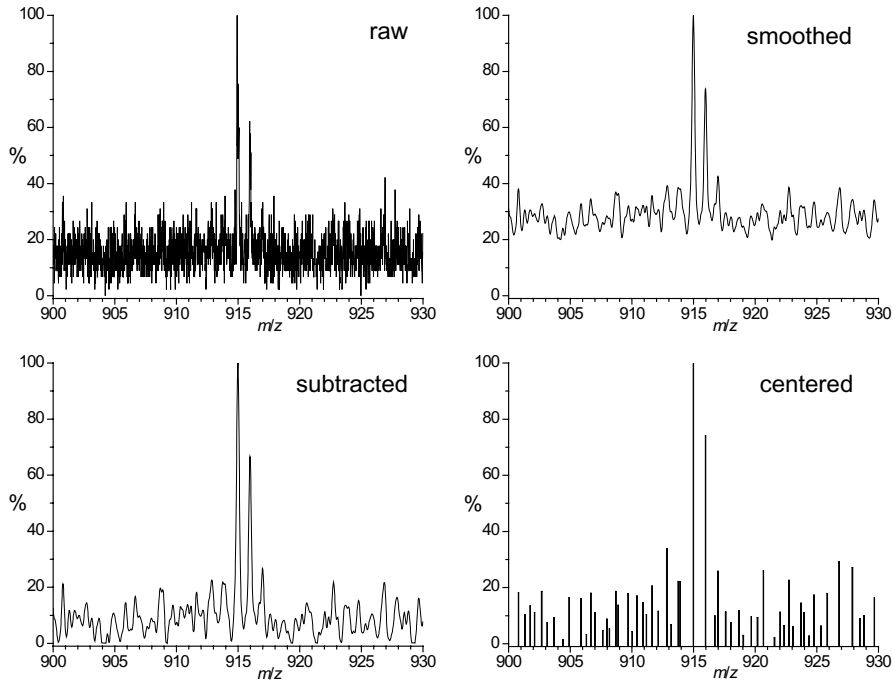

Figure 1.11
Raw data, and its cumulative treatment through smoothing, subtracting the baseline and centering

moving average method, and distortion of the data is less pronounced. However, all smoothing functions inherently lose some of the original information, and are generally applied for cosmetic effect. The *best* way to smooth data is not through mathematical treatment of a single data set, but rather to collect more sets (Figure 1.12).

Repetitive additions of noisy signals tend to emphasise their systematic characteristics and to cancel out random noise, which will average to zero. The signal-to-noise ratio will diminish by a factor of $\sqrt{N}$, where N is the number of repeat scans.

Subtracting

Subtraction essentially adjusts the baseline of the spectrum to equal zero. A variety of polynomial functions can be applied if the baseline is curved. Little information is lost during this process and the resulting mass spectrum is generally easier to interpret, especially when comparing the relative intensities of peaks.

Centering

The process of centering the data involves reducing a peak profile to a single line, indicating the peak centroid and intensity. This has the advantage of greatly reducing the amount of data required to display the spectrum – even in the rather noisy spectrum shown in Figure 1.11, less than $1/30^{th}$ of the amount of information is needed to display the centered spectrum compared to the others. The data compression advantage is less important than it once was, due to tremendous improvements in computer hardware and

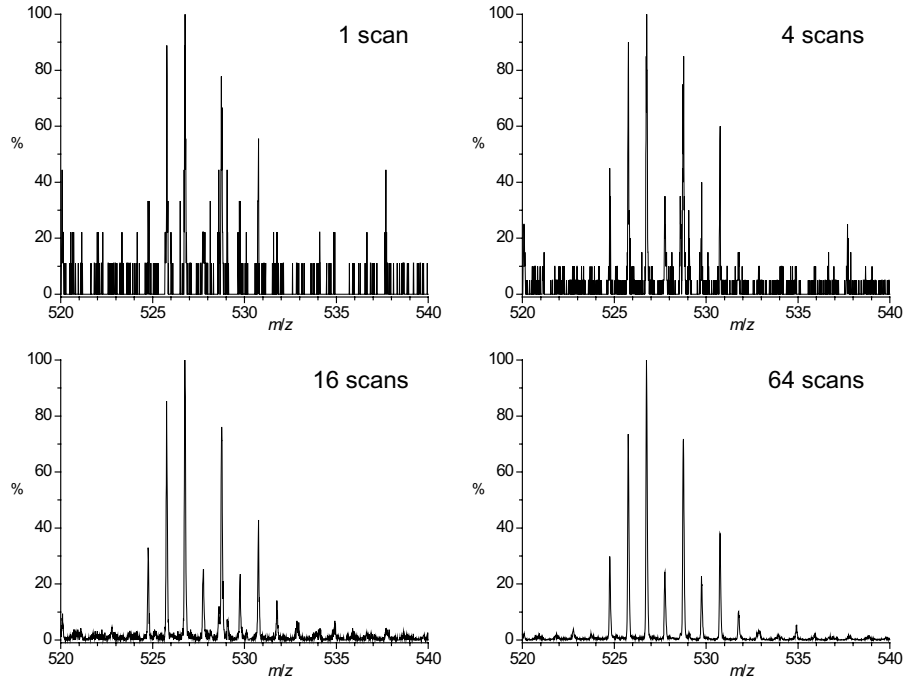

Figure 1.12 The effect of collecting and averaging multiple spectra

data storage. However, centering remains an important precursor to applying computational analysis of the data, such as library searching or instrument calibration.

In general, it is desirable that the raw data that make up a mass spectrum are manipulated as little as possible. The signal-to-noise ratio tells the analyst something about the strength of the signal and hence the quality of the data. Smoothing disguises this indicator, and artificially broadens peaks. Centered data are highly compressed but much information is thrown out, and with today's practically limitless electronic storage this saving may represent a false economy.

1.7 Isotopes

Perhaps the most immediately obvious difference between the mass spectra of organic compounds and those of inorganic and organometallic compounds is the wide occurrence of polyisotopic elements (Appendix 1). A mass spectrometer separates individual ions, so an ion of a given elemental composition containing one or more polyisotopic elements will give rise to a number of **isotope peaks**. These peaks have a characteristic pattern of relative intensities and spacing, which depends on both the masses and the relative abundances of the isotopes in the ion, and this envelope of peaks is known as the **isotope pattern** of an ion.

Spectra of organic compounds generally show rather simple isotope patterns. The reason for this becomes obvious when the isotopic abundances of the elements commonly encountered in organic chemistry are inspected:

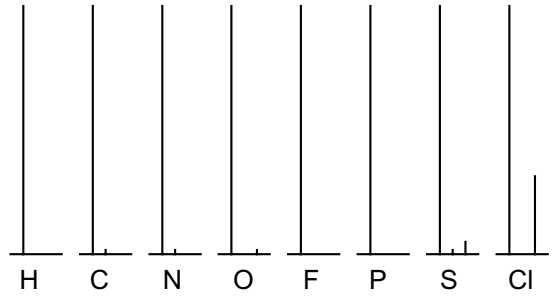

Choosing a part of a row of the heavier elements, the difference is quite striking. Below are the isotopes of elements with atomic numbers 44 to 51:

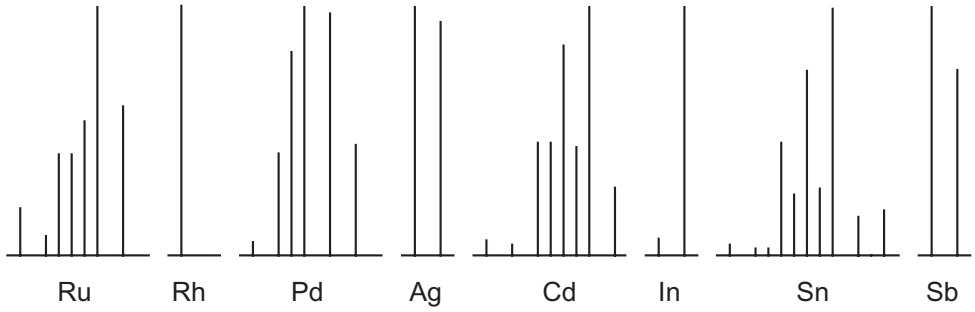

Isotope patterns of polyatomic ions are calculated using the binomial expansion:

$$(a_A.^xA + b_A.^yA + c_A.^zA + \cdots)^n \times (a_B.^xB + b_B.^yB + c_B.^zB + \cdots)^m \times \cdots$$

where a_A, b_A, c_A etc. are the fractional abundances of the isotopes x^A, y^A, z^A of element A and n the number of atoms of A present in the ion; similarly for m atoms of B, and so on. These calculations are accomplished extremely quickly using modern computers, but a simple example is illustrative of the process that goes on.

Example: $[IrCl_2(CO)_2]^-$. Iridium has two isotopes (^{191}Ir 37 %, ^{193}Ir 63 %), as does chlorine (^{35}Cl 76 %, ^{37}Cl 24 %). The contributions of the minor isotopes of carbon (^{13}C, 1 %) and oxygen (^{17}O 0.00038 % and ^{18}O 0.002 %) are negligible in this case. Table 1.1 shows how to calculate the relative abundance of each of the peaks in the isotope pattern and Figure 1.13 plots the resulting pattern.

Table 1.1 Calculating the relative abundance of peaks

Ion composition	*m/z*	Fractional abundance		Relative abundance
$^{191}Ir\ ^{35}Cl_2\ (CO)_2$	317	$(0.37)(0.76)^2$	$= 0.214$	43 %
$^{193}Ir\ ^{35}Cl_2\ (CO)_2$	319	$(0.63)(0.76)^2$	$= 0.364$	100 %
$^{191}Ir\ ^{35}Cl\ ^{37}Cl\ (CO)_2$		$(0.37)(0.76)(0.24) \times 2$*	$= 0.135$	
$^{193}Ir\ ^{35}Cl\ ^{37}Cl\ (CO)_2$	321	$(0.63)(0.76)(0.24) \times 2$*	$= 0.230$	50 %
$^{191}Ir\ ^{37}Cl_2\ (CO)_2$		$(0.37)(0.24)^2$	$= 0.021$	
$^{193}Ir\ ^{37}Cl_2\ (CO)_2$	323	$(0.63)(0.24)^2$	$= 0.036$	7 %

* $\times$ 2 because the ion intensity is made up of contributions from ^{35}Cl ^{37}Cl and ^{37}Cl ^{35}Cl.

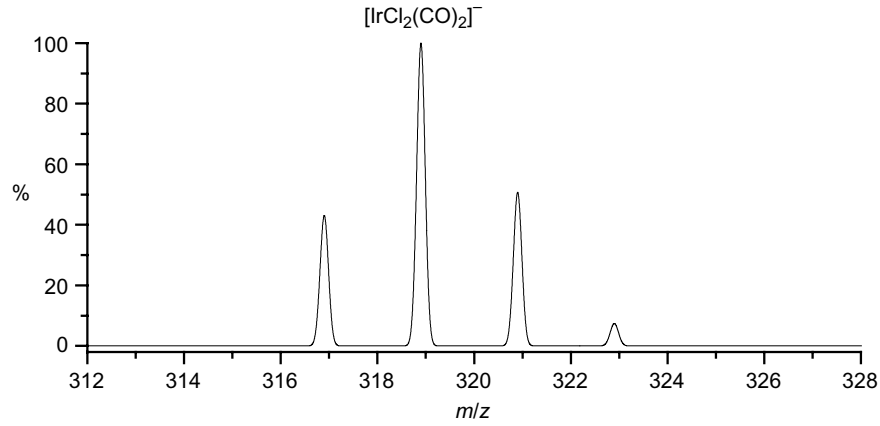

Figure 1.13 Calculated isotope pattern of $[IrCl_2(CO)_2]^-$

Table 1.2 Number of carbon atoms in molecule

	C	C_{10}	C_{25}	C_{50}	C_{90}
M	100	100	100	100	99
M+1	1	11	27	55	100
M+2			3	15	49
M+3				2	16
M+4					3

While the presence of ^{13}C has little effect on the isotope patterns of small ions, in high molecular weight compounds the multiplying effect makes the influence from carbon significant. The effect can be plainly seen in Table 1.2, where the contribution to the $M + n$ peaks increases with the number of carbon atoms, to the point where the $M + 1$ peak has greater intensity than that for M for C_{90}. This effect is particularly significant for large molecules of biological origin such as proteins.

However, the presence of multiple polyisotopic metal atoms has a much more dramatic effect. Compounds with high molecular weights that contain many polyisotopic metal atoms have extremely broad isotope patterns; for example, the hexamer of $SnPh_2$, Sn_6Ph_{12} has a pattern that stretches across more than 30 Da, and has a near-perfect Gaussian distribution of isotope peaks (Figure 1.14).

Most proprietary mass spectrometric software packages come with an isotope pattern calculator. However, there are resources available on the world-wide web to perform these calculations. Online examples (as of 2004) include:

- Mark Winter's[†] isotope patterns calculator at *http://www.shef.ac.uk/chemistry/chemputer/isotopes.html*
- Jonathan Goodman's molecular weight calculator at *http://www.ch.cam.ac.uk/magnus/MolWeight.html*

[†] Mark Winter is also the author of the compendious and reliable WebElements (*http://www.webelements.com/*), *the* online reference for all things related to the periodic table.

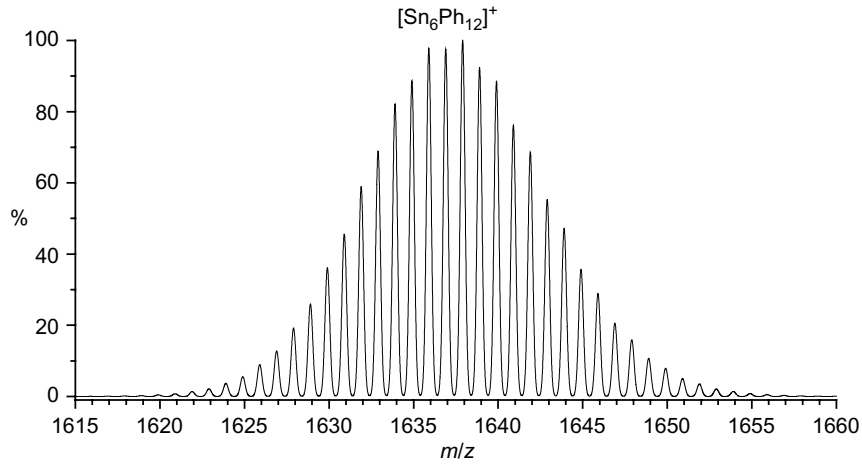

Figure 1.14
Calculated isotope pattern for $[C_{72}H_{60}Sn_6]^+$

- More sophisticated downloadable programs for offline determination of patterns are also available, such as Matthew Monroe's excellent (and free) Molecular Weight Calculator at *http://jjorg.chem.unc.edu/personal/monroe/mwtwin.html*.

1.7.1 Isotopic Abundances of the Elements[16]

The periodic table of the elements colored by number of isotopes (Figure 1.15) demonstrates a distinct alternation, whereby elements with a even atomic number have more isotopes than neighboring odd atomic number elements. Furthermore, cosmic abundances of the elements show the same alternation.

Why? Spin-pairing is an important factor for protons and neutrons, and of the 273 stable nuclei, just four have odd numbers of both protons and neutrons. Elements with even numbers of protons tend to have large numbers of stable isotopes, whereas those

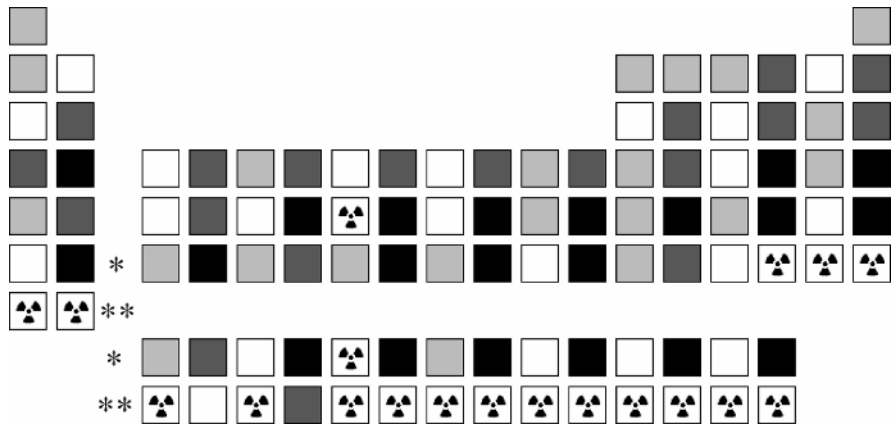

Figure 1.15
The periodic table, coloured by number of stable isotopes. White = 1 isotope, grey = 2, dark grey = 3–5, black = 6+; symbol = all isotopes are radioactive. See Appendix 2 for a more detailed version

with odd numbers of protons tend to have one, or at most two, stable isotopes. For example, $_{52}$Te has eight stable isotopes and $_{54}$Xe has nine but $_{53}$I has just one.

An additional feature is the existence of especially stable numbers of nucleons of one kind, and these '**magic numbers**' are 2, 8, 20, 28, 50, 82 and 126. These numbers correspond to completed quantum levels for the nuclei, and just like for electrons these confer particular stability (though the order in which the levels are filled differ for nuclei). Patterns among the stable isotopes bear this extra stability out. For example, tin (50 protons) has the greatest number of stable isotopes (10); lead (82 protons) isotopes are the end result of all decay pathways of the naturally occurring radioactive elements beyond lead; seven elements include isotopes with 82 neutrons (**isotones** ^{136}Xe, ^{138}Ba, ^{139}La, ^{140}Ce, ^{141}Pr, ^{142}Nd and ^{144}Sm) and six elements have isotopes with 50 neutrons (^{86}Kr, ^{87}Rb, ^{88}Sr, ^{89}Y, ^{90}Zr and ^{92}Mo). Similarly, 'doubly-magic' nuclei are strongly favoured: ^{4}He (2 p, 2 n) is the second-most common isotope in the universe, and **α-particles** (helium nuclei) are frequently ejected in nuclear reactions; ^{16}O (8 p, 8 n) makes up 99.8 % of all oxygen, ^{40}Ca (20 p, 20 n) is 97 % abundant, and ^{208}Pb (82 p, 126 n) is the most common isotope of lead. As the atomic number increases, the number of neutrons required to provide stability to the nucleus increases at a greater rate (Figure 1.16). The plotted points represent the naturally occurring isotopes; careful inspection reveals the extra stability of spin-paired nuclei.

The precision to which the **atomic weight** is known for any given element is related to the number of isotopes an element has. Generally, the atomic weight of any given isotope can be determined experimentally using mass spectrometry to an extremely high level. Gold, for example, has a single stable isotope (^{197}Au) whose relative atomic mass is 196.96655(2). However, the relative abundances of the various isotopes of a polyisotopic element are known to a lower level of precision. Mercury has seven stable isotopes, and its relative atomic mass is 200.59(2) (i.e. five significant figures compared to eight

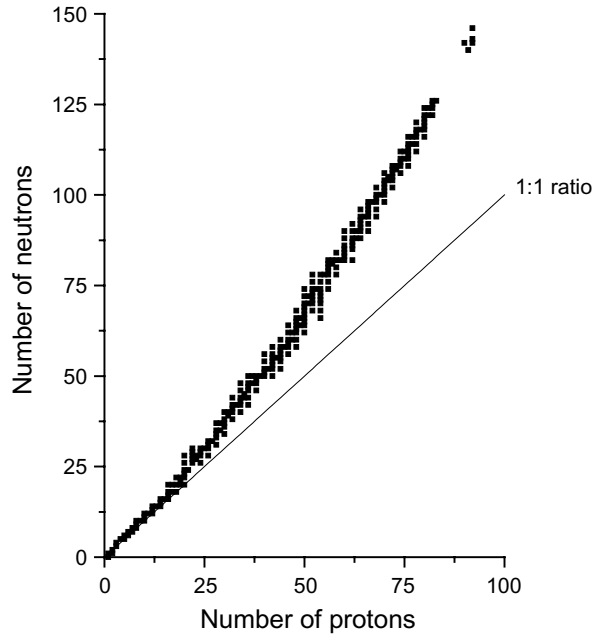

Figure 1.16
Plot of neutron number vs. proton number for the naturally occurring isotopes

significant figures for gold). Furthermore, relative isotopic abundances can depend on the source of the sample, and this phenomenon is the basis of stable isotope geochemistry. Mass spectrometry can, for example, easily detect the difference between carbon dioxide exhaled by humans from that generated by burning coal by analysing the $^{12}C/^{13}C$ ratio. Similar studies are done on $^{14}N/^{15}N$ and $^{16}O/^{18}O$ ratios.[17]

Another complication can arise from **isotopic enrichment** of samples. Most notably, this is performed on uranium ore to obtain ^{235}U for use as a nuclear fuel, leaving **depleted** uranium behind as predominantly ^{238}U, and it is this isotope that generally finds itself in chemistry laboratories. In the middle of the last century, 'strategic lithium', ^{6}Li, was stockpiled for use in nuclear weapons and as a raw material for the production of tritium (itself used in nuclear weapon production). The depleted lithium, predominantly ^{7}Li, was sold on and this had a noticeable effect on the atomic weight of some supplies of lithium. The International Union for Pure and Applied Chemistry (IUPAC) publishes periodic reports on the history, assessment and continuing significance of atomic weight determinations.[18]

1.7.2 Isotope Pattern Matching

Comparisons between theoretical and experimental isotope patterns are often done by eye, but a direct comparison is highly recommended. This approach enables direct matching between each member of the isotope pattern. Using the proprietary mass spectrometer software provides an easy way of achieving this, simply by presenting the two spectra overlaid (Figure 1.17).

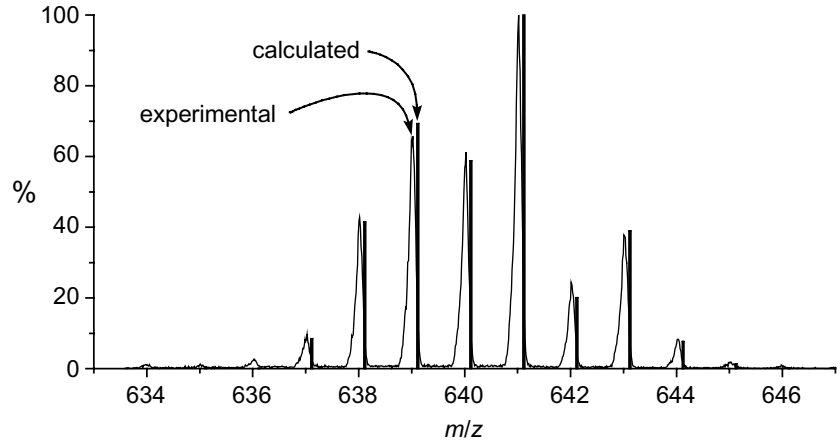

Figure 1.17 Experimental (line) and calculated (bar) isotope patterns for $[Yb(EDTA)(HMPA)]^-$

Immediately apparent in the example is the fact that the calibration is off by approximately 0.1 *m/z*, but the match between experimental and calculated patterns is good. In cases as clear-cut as this one, assignment made be made with confidence. Difficulties tend to arise in the following examples:

(a) Signal-to-noise ratio is low. This can cause the lower intensity peaks of the isotope pattern to disappear into the noise. The best remedy is to sum many scans over a small window, and if the signal is very weak this may take minutes.

(b) Resolution is low. This can cause the peaks to overlap, and is particularly problematic for multiply charged species of high molecular weight. Many instruments can trade-off sensitivity for resolution, and this approach is always recommended especially if the signal is a strong one.

(c) Calibration is poor. Easily remedied by recalibrating the instrument; there is generally no need to rerun the sample as most software allows spectra to be calibrated retrospectively.

(d) Two patterns overlap when two ionisation pathways are competing, for example between oxidation to form $[M]^{\bullet+}$ (for example, as occurs with certain ferrocene derivatives, see Section 7.4.1) and protonation to form $[M + H]^+$ or the appearance of $[M + NH_4]^+$ and $[M + H + H_2O]^+$. Rather than trying to deconvolute the overlapping isotope patterns, the best approach is promote one ionisation pathway at the expense of the other (e.g. add extra H^+) or to look for another ionisation route altogether. If solvent adducts are present, application of gentle in-source CID should remove this complication.

(e) Two patterns overlap from different compounds. In organometallic and coordination chemistry this case is certainly rarer than in organic chemistry, but the latter has the advantage that chromatographic separation is always an option (LCMS or GCMS). However, it may happen; for example in a mixture of lanthanide complexes (which

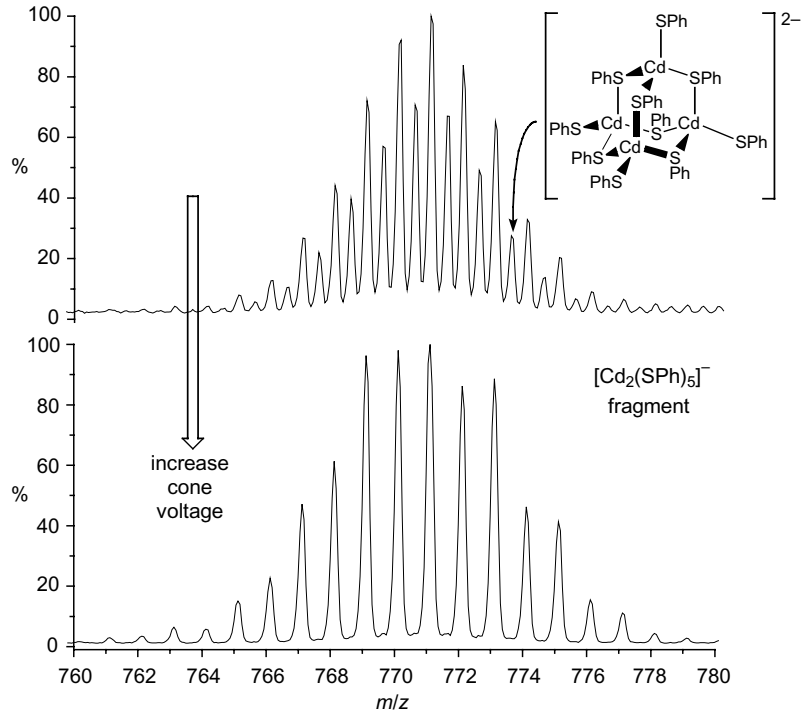

Figure 1.18
Top spectrum (ESI-MS, negative-ion mode) shows the overlapping isotope patterns of $[Cd_4(SPh)_{10}]^{2-}$ and its symmetrical fragment ion $[Cd_2(SPh)_5]^-$.[19] Increasing the cone voltage (in-source CID) removes the intact parent ion completely (bottom spectrum). The same strategy can be used to produce $[M]^{+/-}$ from its dimer, $[2M]^{2+/-}$

have very similar chemistry and whose isotope patterns frequently overlap with their neighbours). If the two components can be identified separately the isotope patterns can be calculated and combined in the appropriate proportion to model the experimentally observed pattern. Overlap of patterns when both components are unknown can be very difficult to unravel, and sample purification before reanalysis is probably the best way to proceed.

(f) Two patterns overlap where one is from $[M]^{+/-}$ and another from the dimer, $[2M]^{2+/-}$. For polyisotopic species, the presence of the dimer is obvious from the isotope pattern, because there will be peaks separated by 0.5 *m/z*. Symmetrical fragmentation of a doubly-charged ion has the same effect. Again, in-source CID can simplify the picture (Figure 1.18).

References

1. K. R. Jennings, *Int. J. Mass Spectrom.*, 2000, **200**, 479; A. K. Shukla and J. H. Futrell, *J. Mass Spectrom.*, 2000, **35**, 1069; E. de Hoffmann, *J. Mass Spectrom.*, 1996, **31**, 129; K. L. Busch, G. L. Glish and S. A. McLuckey, *Mass Spectrometry/Mass Spectrometry: Techniques and Applications of Tandem Mass Spectrometry*, VCH, New York, 1988.
2. R. A. Yost and C. G. Enke, *J. Am. Chem. Soc.*, 1978, **100**, 2274.
3. K. M. Ervin, *Chem. Rev.*, 2001, **101**, 391; P. B. Armentrout, *Acc. Chem. Res.*, 1995, **28**, 430; B. S. Freiser, *Acc. Chem. Res.*, 1994, **27**, 353.
4. see P. B. Armentrout, *Int. J. Mass Spectrom.*, 2003, **227**, 289, and 80+ references to this group's work therein; R. Amunugama and M. T. Rodgers, *Int. J. Mass Spectrom.*, 2003, **227**, 1.
5. F. Muntean and P. B. Armentrout, *J. Chem. Phys.*, 2001, **115**, 1213.
6. R. Liyanage, M. L. Styles, R. A. J. O'Hair and P. B. Armentrout, *Int. J. Mass Spectrom.*, 2003, **227**, 47.
7. R. A. Forbes, L. Lech and B. S. Freiser, *Int. J. Mass Spectrom. Ion Proc.*, 1987, **77**, 107; C. E. C. A. Hop, T. B. McMahon and G. D. Willett, *Int. J. Mass Spectrom. Ion Proc.*, 1990, **101**, 191; J. B. Westmore, L. Rosenberg, T. S. Hooper, G. D. Willett and K. J. Fisher, *Organometallics,* 2002, **21**, 5688.
8. A. G. Harrison, *Rapid Commun. Mass Spectrom.*, 1999, **13**, 1663.
9. P. J. Dyson, B. F. G. Johnson, J. S. McIndoe and P. R. R. Langridge-Smith, *Rapid Commun. Mass Spectrom.*, 2000, **14**, 311; P. J. Dyson, A. K. Hearley, B. F. G. Johnson, J. S. McIndoe, P. R. R. Langridge-Smith and C. Whyte, *Rapid Commun. Mass Spectrom.*, 2001, **15**, 895; C. P. G. Butcher, P. J. Dyson, B. F. G. Johnson, P. R. R. Langridge-Smith, J. S. McIndoe and C. Whyte, *Rapid Commun. Mass Spectrom.*, 2002, **16**, 1595.
10. P. J. Dyson, A. K. Hearley, B. F. G. Johnson, T. Khimyak, J. S. McIndoe and P. R. R. Langridge-Smith, *Organometallics*, 2001, **20**, 3970.
11. A. W. T. Bristow and K. S. Webb, *J. Am. Soc. Mass Spectrom.*, 2003, **14**, 1086.
12. A. N. Tyler, E. Clayton and B. N. Green, *Anal. Chem.*, 1996, **68**, 3561.
13. J. E. Deline, *Molecular Fragment Calculator 1.0*, 1995.
14. J. S. McIndoe and B. K. Nicholson, *Acta Cryst. Sect. E,* 2002, **E58**, m53.
15. A. Savitsky and M. J. E. Golay, *Anal. Chem.*, 1964, **36**, 1627.
16. P. A. Cox, *The Elements,* Oxford University Press, Oxford, 1989.
17. R. Corfield, *Chem. Brit.,* 2003, **39**, 23.
18. J. R. de Laeter, J. K. Böhlke, P. de Bièvre, H. Hidaka, H. S. Peiser, K. J. R. Rosman and P. D. P. Taylor, *Pure Appl. Chem.*, 2003, **73**, 683.
19. T. Løver, W. Henderson, G. A. Bowmaker, J. Seakins and R. P. Cooney, *Inorg. Chem.*, 1997, **36**, 3711.